

DTIC FILE COPY

2

GL-TR-90-0059

ENVIRONMENTAL RESEARCH PAPERS, NO. 1058

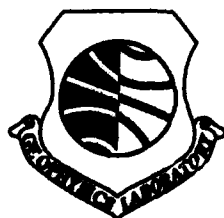
# Tests of a Mesoscale Model Coupled With a Boundary Layer/Soil Model

GEORGE D. MODICA

AD-A227 322



26 March 1990



DTIC  
ELECTE  
OCT 11 1990  
S B D  
Ca

Approved for public release; distribution unlimited.

ATMOSPHERIC SCIENCES DIVISION

PROJECT 2310

## GEOPHYSICS LABORATORY

HANSCOM AFB, MA 01731-5000

90-10-09 124

"This technical report has been reviewed and is approved for publication"

FOR THE COMMANDER



DONALD A. CHISHOLM, Chief  
Atmospheric Prediction Branch



ROBERT A. MCCLATCHEY, Director  
Atmospheric Sciences Division

This document has been reviewed by the ESD Public Affairs Office (PA) and is releasable to the National Technical Information Service (NTIS).

Qualified requestors may obtain additional copies from the Defense Technical Information Center. All others should apply to the National Technical Information Service.

If your address has changed, or if you wish to be removed from the mailing list, or if the addressee is no longer employed by your organization, please notify GL/DAA, Hanscom AFB, MA 01731. This will assist us in maintaining a current mailing list.

# REPORT DOCUMENTATION PAGE

Form Approved  
OMB No. 0704-0188

Public reporting for this collection of information is estimated to average 1 hour per response, including the time for reviewing instructions, searching existing data sources, gathering and maintaining the data needed, and completing and reviewing the collection of information. Send comments regarding this burden estimate or any other aspect of this collection of information, including suggestions for reducing this burden, to Washington Headquarters Services, Directorate for Information Operations and Reports, 1215 Jefferson Davis Highway, Suite 1204, Arlington, VA 22202-4302, and to the Office of Management and Budget, Paperwork Reduction Project (0704-0188), Washington, DC 20503.

1. AGENCY USE ONLY (Leave blank)		2. REPORT DATE 26 March 1990		3. REPORT TYPE AND DATES COVERED Scientific, Interim (01 Oct 88 to 30 Sep 89)	
4. TITLE AND SUBTITLE Tests of a Mesoscale Model Coupled with a Boundary Layer/Soil Model				5. FUNDING NUMBERS PE 62101F PR 2310 TA G7 WU 10	
6. AUTHOR(S) Modica, George D.					
7. PERFORMING ORGANIZATION NAME(S) AND ADDRESS(ES) Geophysics Laboratory (LYP) Hanscom Air Force Base Massachusetts 01731-5000				8. PERFORMING ORGANIZATION REPORT NUMBER GL-TR-90-0059 ERP, No. 1058	
9. SPONSORING/MONITORING AGENCY NAME(S) AND ADDRESS(ES)				10. SPONSORING/MONITORING AGENCY REPORT NUMBER	
11. SUPPLEMENTARY NOTES					
12a. DISTRIBUTION/AVAILABILITY STATEMENT Approved for public release; distribution unlimited				12b. DISTRIBUTION CODE	
13. ABSTRACT (Maximum 200 words) A meso-beta grid point model with a detailed microphysics parameterization of warm-cloud processes is briefly described. The model is initialized with a mesoscale data set beginning 12Z on 27 March 1982 at a location centered over north-central Texas. Parameters from subsequent 6-h forecasts are compared with observations. Velocity, temperature and moisture parameters generally appeared to be forecast well. The model was additionally run without any PBL/soil model physics to evaluate the effect that these processes have on the forecast. The most noticeable effects were observed near the surface where forecast temperatures were too cold and winds were too high. This run also yielded about 20-50 percent less precipitation. The model's soil physics parameterization appears to be essential to represent realistically the supply to the lower atmosphere of the moisture necessary for the precipitating clouds. Sensitivity tests with the PBL/soil model revealed that, at least for this case, the effect of soil moisture on ground temperature is approximately as important as the effect of clouds on ground temperature. However, when the effects of clouds were removed from the model atmosphere, the ground temperature and PBL height tended to exhibit unusual oscillations. The reasons for this are not yet known.					
14. SUBJECT TERMS Numerical weather prediction Boundary layer models Mesoscale models Cloud forecasting				15. NUMBER OF PAGES 48	
				16. PRICE CODE	
17. SECURITY CLASSIFICATION OF REPORT Unclassified	18. SECURITY CLASSIFICATION OF THIS PAGE Unclassified	19. SECURITY CLASSIFICATION OF ABSTRACT Unclassified	20. LIMITATION OF ABSTRACT SAR		

## Preface

I would like to express my gratitude to those who helped to make this report possible: Mr. Sam Yee for his careful guidance and helpful suggestions; Mr. Artie Jackson for giving me the data set used in this study; Dr. H. Stuart Muench for comments and suggestions.

Accession For	
NTIS GRA&I	<input checked="" type="checkbox"/>
DTIC TAB	<input type="checkbox"/>
Unannounced	<input type="checkbox"/>
Justification	
By	
Distribution/	
Availability Codes	
Dist	Avail and/or Special
A-1	

## Contents

1. INTRODUCTION	1
2. NUMERICAL MODEL	2
3. INITIAL DATA	3
4. RESULTS OF 6-HOUR SIMULATIONS	7
5. SUMMARY AND CONCLUSIONS	37
REFERENCES	39

## Illustrations

1. Surface Pressure Over US for 12Z 27 March 1982	4
2. 500 mb Mesoscale Analysis for 12Z 27 March 1982	5
3. Gridded Terrain Height (m) for Model Domain	6
4. Horizontal Plot of Forecast and Observed Winds at Sigma-Level 0.9978	8
5. Horizontal Plot of Forecast and Observed 850 mb Winds	9
6. Horizontal Plot of Forecast and Observed 500 mb Winds	10
7. Horizontal Plot of Forecast and Observed 300 mb Winds	11
8. Vertical Cross Section of Forecast and Observed U-Wind Component	13
9. Vertical Cross Section of Forecast and Observed V-Wind Component	14
10. Horizontal Plot of Forecast and Observed Geopotential Height and Temperature at Sigma-Level 0.9978	16
11. Horizontal Plot of Forecast and Observed Geopotential Height and Temperature at 850 mb	17
12. Horizontal Plot of Forecast and Observed Geopotential Height and Temperature at 500 mb	18
13. Horizontal Plot of Forecast and Observed Geopotential Height and Temperature at 300 mb	19
14. Vertical Cross Section of Forecast and Observed Potential Temperature	21
15. Horizontal Plot of Forecast and Observed Vapor Mixing Ratio at Sigma-Level 0.9978	23
16. Horizontal Plot of Forecast and Observed Vapor Mixing Ratio at 850 mb	24

17. Horizontal Plot of Forecast and Observed Vapor Mixing Ratio at 500 mb	25
18. Vertical Cross Section of Forecast and Observed Vapor Mixing Ratio	26
19. Vertical Cross Section of Forecast Cloud Water Mixing Ratio	27
20. Horizontal distribution of Forecast and Observed Precipitation	28
21. Horizontal Plot of Forecast and Observed Wind at Sigma-Level 0.9978 for Non-PBL Case	30
22. Horizontal Plot of Forecast Geopotential Height and Temperature at Sigma-Level 0.9978 for Non-PBL Case	31
23. Horizontal Plot of Forecast Precipitation for Non-PBL Case	32
24. Horizontal Plot of Forecast Vapor Mixing Ratio at Sigma-Level 0.9978 for Non-PBL Case	33
25. Vertical Cross Section of Forecast Cloud Water Mixing Ratio for Non-PBL Case	34
26. Plot of Ground Temperature and PBL Height vs. Time for Various Experiments	36

# TESTS OF A MESOSCALE MODEL COUPLED WITH A BOUNDARY LAYER/SOIL MODEL

## 1. INTRODUCTION

Recent Increases in computer power have made feasible the use of numerical weather prediction (NWP) models for resolving and studying mesoscale physical processes within limited-area domains. Atmospheric modeling has progressed to such a point that we are now increasingly focusing on the realistic simulation and prediction of the so-called 'observable weather.' In many cases, this means mesoscale phenomena largely confined to the planetary boundary layer and typically with temporal scales of less than 6 hours and spatial scales of less than 100 kilometers. To realistically simulate/predict such phenomena, we must emphasize the parameterization of the diurnal variations in the planetary boundary layer. With this in mind, we have coupled a limited-area model with a soil/boundary-layer model to study the effect of the forcing due to sources and sinks of moisture and heat at the earth-atmosphere interface on mesoscale phenomena. This report represents a summary of our progress along two fronts: 1) to assure that the coupled mesoscale model/PBL/soil model behaves realistically in a general sense; 2) to experiment with the PBL/soil model parameterization in a way that reveals information about mesoscale weather events.

Section 2 contains a description of the mesoscale model. Section 3 describes the initial data and analysis techniques used to create input fields for the model. Some model forecast

---

(Received for publication 23 March 1990)



results are presented and discussed in Section 4. Finally, Section 5 contains some conclusions of this effort.

## 2. NUMERICAL MODEL

The model is a modified version of the one developed at the National Oceanic and Atmospheric Administration's Environmental Research Laboratory.<sup>1,2</sup> This model is a primitive equation, hydrostatic model that uses a modified sigma coordinate in the vertical and the Arakawa B grid in the horizontal. There are 27 grid points for the wind fields and 26 grid points for mass field variables in each horizontal direction. For tests described here, grid spacing was set to 20 km resulting in a domain size of 500 km  $\times$  500 km. There are 16 vertical layers extending from the surface to 100 mb, with several layers in the lowest kilometer.

The prognostic variables are written in flux form for  $u$ ,  $v$ , equivalent potential temperature, surface pressure, total water mixing ratio (water vapor plus cloud water), rain water mixing ratio, and rain water drop concentration. The model physics include detailed microphysical parameterizations of grid-scale warm cloud processes. Presently, there is no convection parameterization in the model. Planetary boundary layer (PBL) processes are parameterized by first-order closure.<sup>3</sup> The PBL model is coupled with an active two-layer soil model and a primitive plant canopy model.<sup>4</sup> Both soil temperature and moisture are predicted by the soil model; canopy water content is predicted by a plant canopy model.

Time integration is accomplished using the explicit leap-frog scheme with an Asselin filter. The Asselin filter coefficient is set to 0.02 and the model time-step is 20 sec. An explicit horizontal diffusion is included for each prognostic variable (except surface pressure) with the background eddy viscosity set at  $3.0 \times 10^4$  m<sup>2</sup>/sec. The coriolis parameter is constant and has a value of  $f = 7.8 \times 10^{-5}$  sec. The gridded terrain field for the lower boundary of the model was obtained through interpolation of 1 degree terrain data archived at the Defense Mapping Agency.

A sponge boundary scheme is used in the model for the lateral boundary conditions.<sup>5</sup> The scheme used in this model assimilated at the lateral boundaries the objectively analyzed

---

<sup>1</sup> Nickerson, E. C. (1979) On the numerical simulation of airflow and clouds over mountainous terrain, *Bett. Atmos. Phys.*, **52**:161-177.

<sup>2</sup> Nickerson, E. C., Richard, E., Rosset, R. and Smith, D. R. (1986) The numerical simulation of clouds, rain, and airflow over the Vosges and Black Forest Mountains: A meso-beta model with parameterized microphysics, *Mon. Wea. Rev.*, **114**:399-414.

<sup>3</sup> Troen, I. and Mahrt, L. (1986) A simple model of the atmospheric boundary layer; sensitivity to surface evaporation, *Bound. -Layer Meteor.*, **37**:129-148.

<sup>4</sup> Pan, H. -L. and Mahrt, L. (1987) Interaction between soil hydrology and boundary layer development, *Bound. -Layer Meteor.*, **38**:185-202.

<sup>5</sup> Perkey, D. J. and Kreitzberg, C. W. (1976) A time-dependent lateral boundary scheme for limited-area primitive equation models, *Mon. Wea. Rev.*, **104**:744-755.

observed values from the high resolution data set.<sup>6</sup> These values were determined by a linear-in-time interpolation between each three-hour observing period.

### 3. INITIAL DATA

The data used for input to the numerical model were collected during AVE/VAS (Atmospheric Variability Experiment/Vertical Atmospheric Sounder) III day of 27 March 1982. These data consisted of up to twenty-one 3-hourly raobs and over forty hourly surface observations, each located within an area approximately 770 km  $\times$  770 km situated over north central Texas and southern Oklahoma. During this period, there was a strong surface high pressure system centered over Lake Superior (Figure 1). The domain chosen for the mesoscale is centered near Dallas-Ft. Worth, Texas. The conditions at 500 mb are shown in Figure 2. In the Texas-Oklahoma vicinity, the low-level winds were easterly and since the underlying terrain in this region rises from east to west (Figure 3), this could be considered to be an upslope precipitation event.

Observed values of  $u$ ,  $v$ ,  $T$ , and  $q_v$  at 12, 15, and 18Z on 27 March 1982 were analyzed using a blended analysis technique.<sup>7</sup> This blending technique attempts to exploit the complementary nature of high vertical resolution rawinsonde data and high horizontal and temporal resolution surface reports. No balancing of the mass and wind fields was done, although the vertically integrated mass divergence was eliminated from the initial wind field data.<sup>8</sup>

Initial values of soil moisture and soil temperature were specified as functions of the respective relative humidity and temperature of the near-surface air.

---

<sup>6</sup> Barnes, S. L. (1973) *Mesoscale objective analysis using weighted time-series observations*, NOAA Tech. Memo ERL NSSL-62.

<sup>7</sup> Yee, S. Y.-K. and Jackson, A. (1988) *Blending of surface and rawinsonde data in mesoscale objective analysis*, AFGL-TR-88-0144, ADA 203984.

<sup>8</sup> Washington, W. M. and Baumhefner, D. P. (1975) A method for removing Lamb waves from initial data for primitive equation models. *J. Appl. Meteo.* 14:114-119.



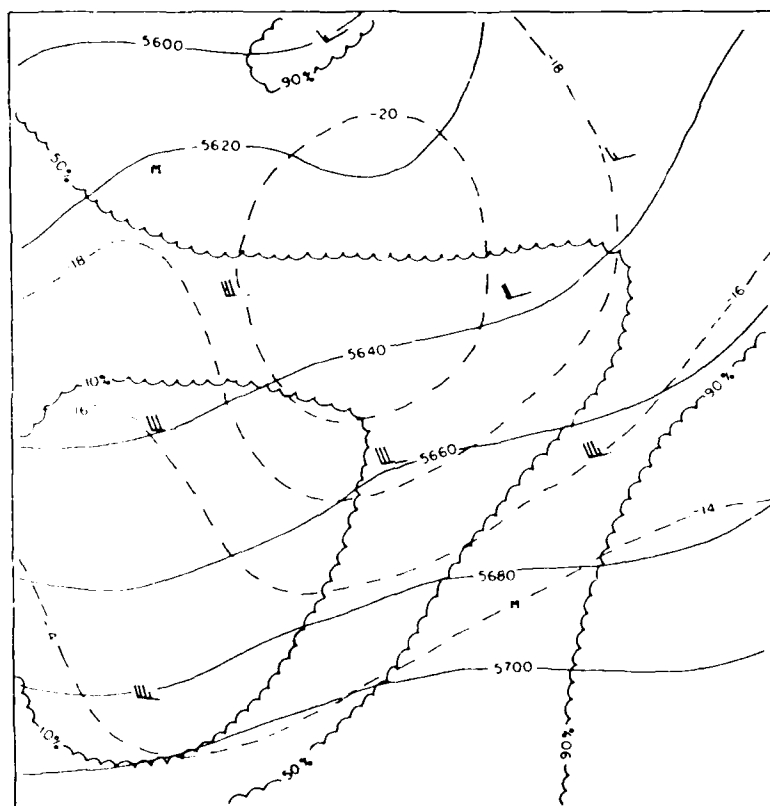


Figure 2. 500 mb Mesoscale Analysis Valid 12Z 27 Mar 82: Height (Solid, in m), Temperature (Dashed, in C), Relative Humidity (Scalloped), and Wind (Each Full Barb Equals 10 m/sec). Stations marked M reported temperature and humidity but not wind.

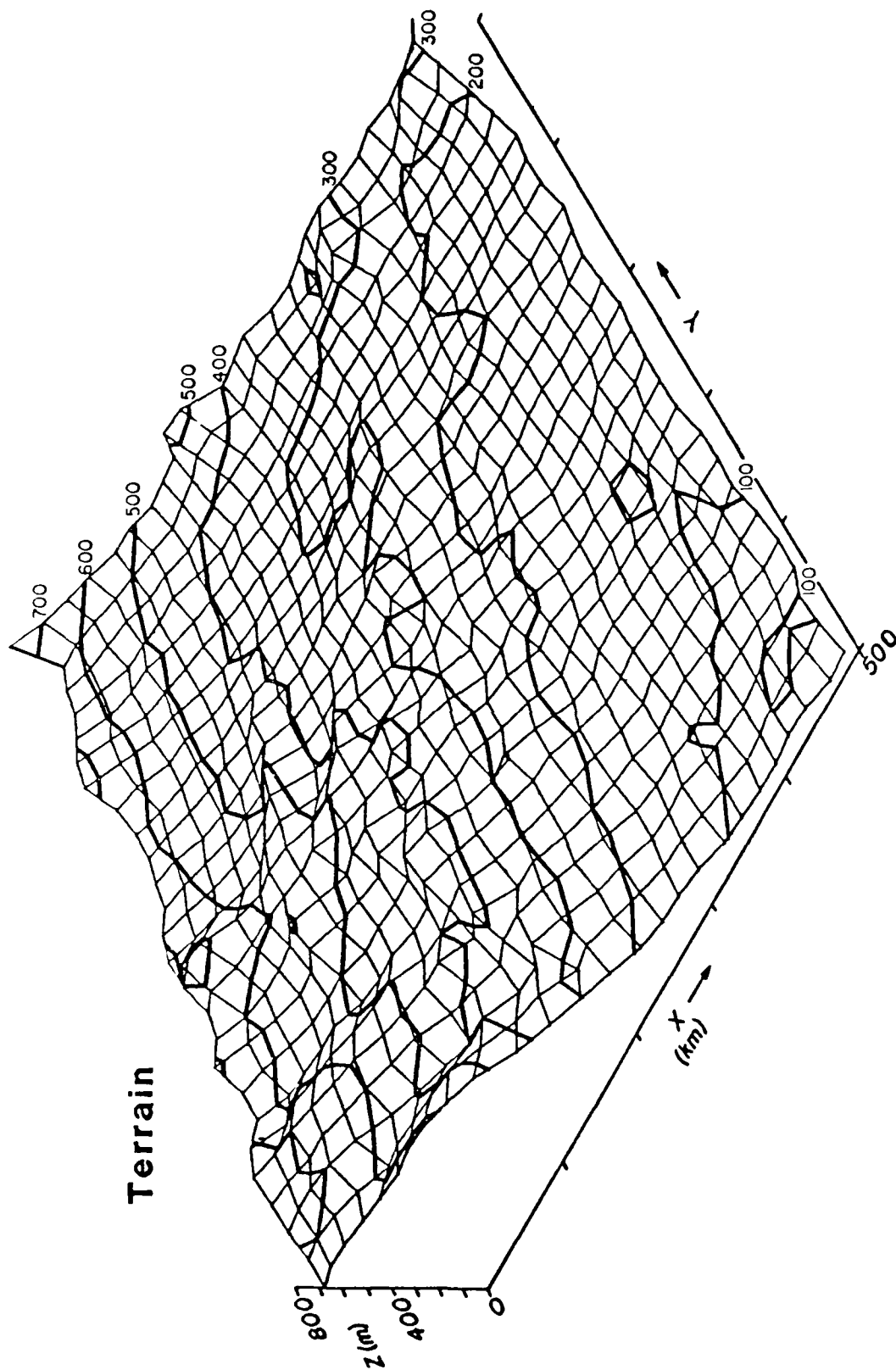
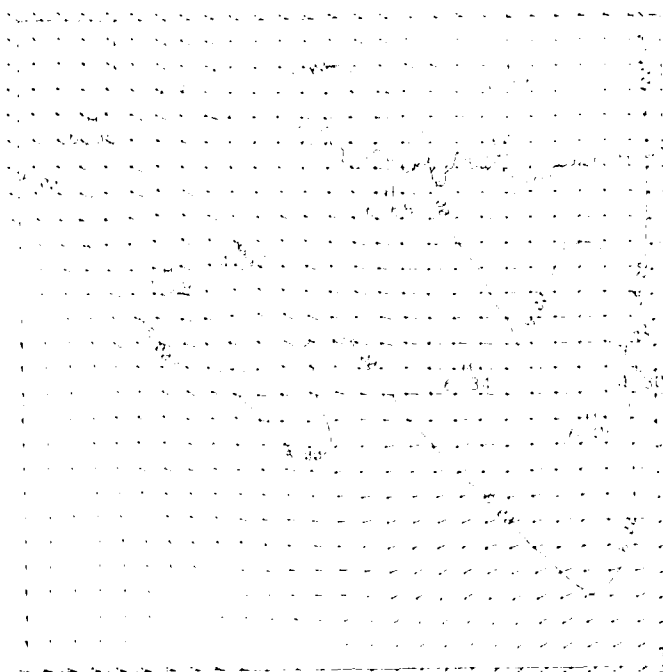


Figure 3. Gridded Terrain Height (m) for Model Domain

#### 4. RESULTS OF 6-HOUR SIMULATIONS

In this section, we compare the 6-h forecast from the model to the objectively analyzed radiosonde data that are valid for the same time.

Figure 4 shows a horizontal plot of the forecast winds. This is at the model's first computational level above the ground (about 16 m). Hereafter, this level will be referred to as level 0.9978 which is the value of the nondimensional vertical coordinate. The model forecast winds are shown in Figure 4a and the actual observed winds are shown in Figure 4b. The forecast winds at this level are too light in both the northeast and southwest corners. There is evidence of a decoupled model solution at the eastern boundary in Figure 4a. In Figure 5a, note that model forecast winds at 850 mb also depart somewhat from the analysis (see Figure 5b). In the central portion of the domain the forecast southerly winds are generally too strong. At mid- and upper-levels of the model (500 and 300 mb; Figures 6 and 7, respectively), there is generally good agreement between the forecast and observed wind fields except in the northwest corner at 300 mb.



**Figure 4a.**

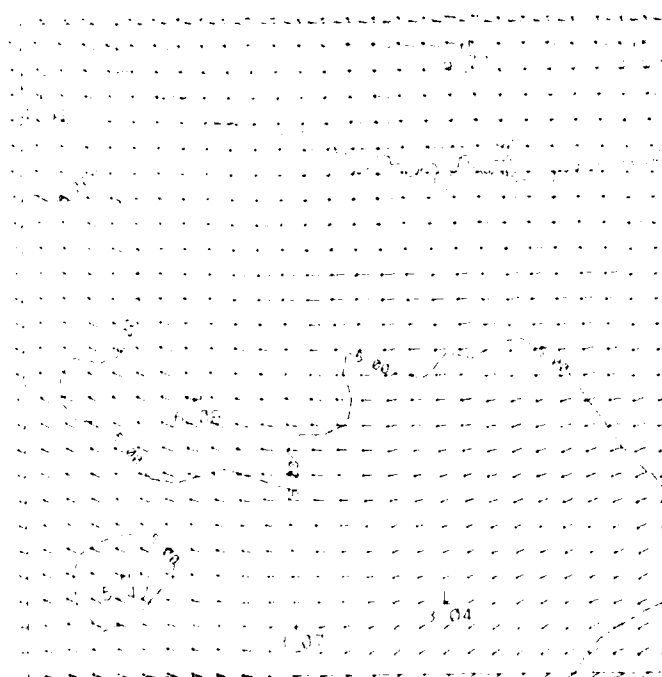


**Figure 4b.**

**Figure 4. Horizontal Plot of 6-h (a) Forecast and (b) Observed, Wind (m/sec) at Sigma-Level 0.9978 Valid 18Z 27 Mar 82**

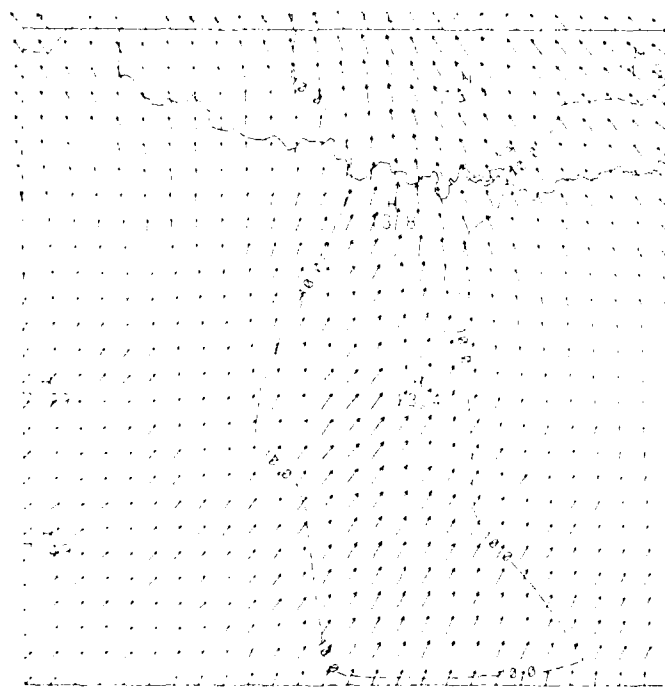


Figure 5a.

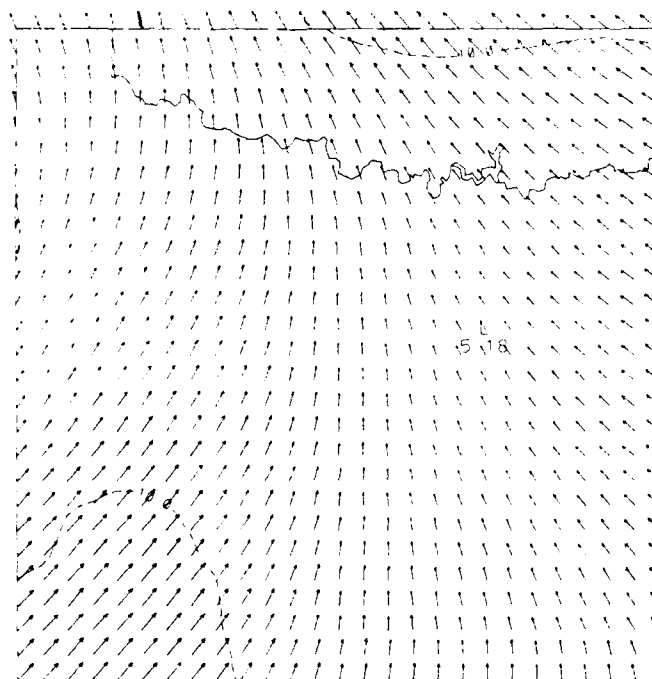


Figure 5b.

Figure 5. Horizontal Plot of 6-h (a) Forecast and (b) Observed, Wind (m/sec) at 850 mb Valid 18Z 27 Mar 82



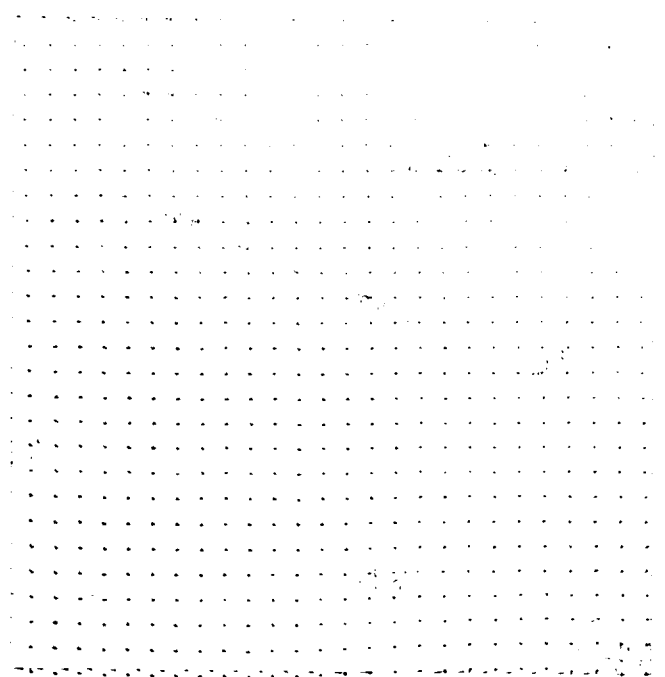


Figure 6a.

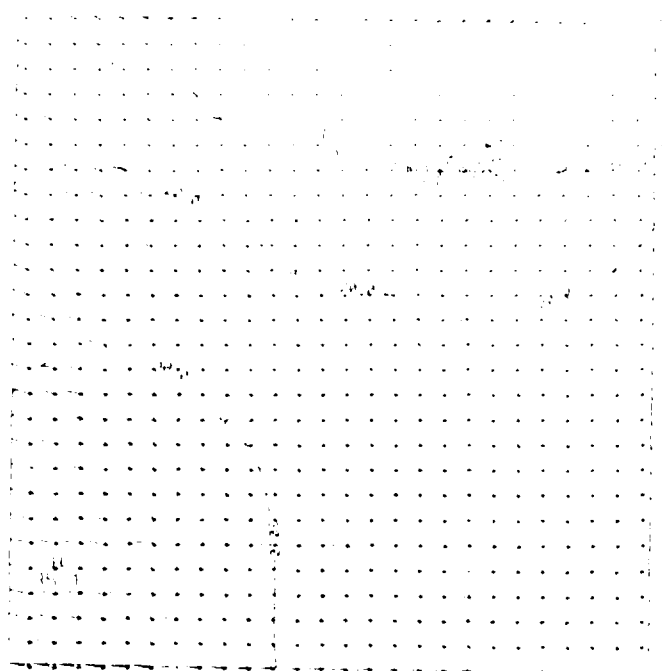


Figure 6b.

Figure 6. Horizontal Plot of 6-h (a) Forecast and (b) Observed, Wind (m/sec) at 500 mb Valid 18Z 27 Mar 82

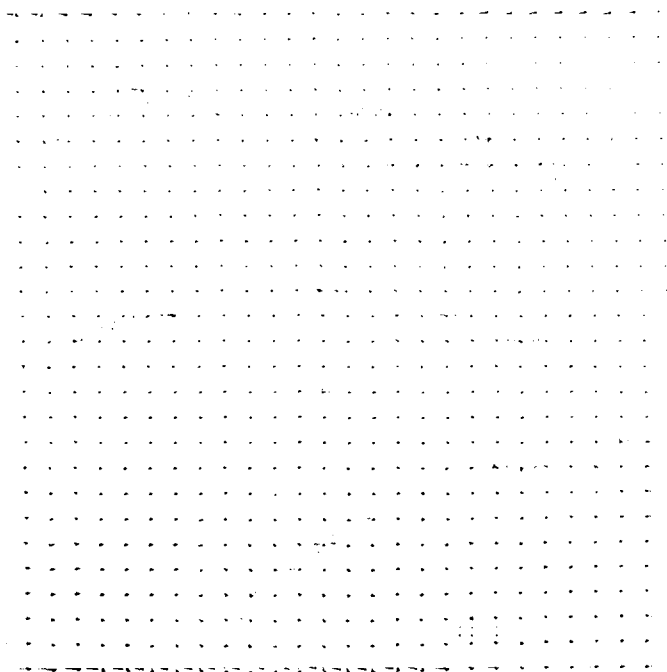


Figure 7a.

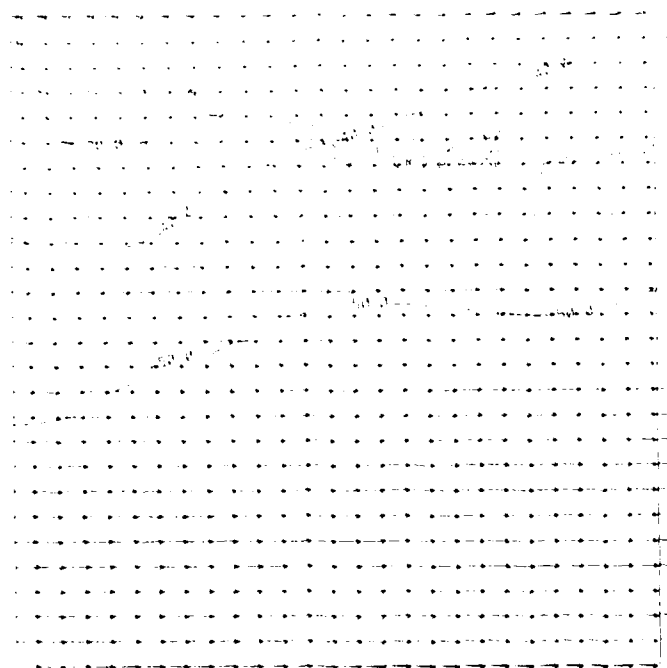


Figure 7b.

Figure 7. Horizontal Plot of 6-h (a) Forecast and (b) Observed, Wind (m/sec) at 300 mb Valid 18Z 27 Mar 82

Figure 8 shows a west-to-east cross section of the u-wind component centered midway between the northern and southern extent of the model domain. The model forecast (Figure 8a) places the 0 m/sec isotach at about 900-850 mb so that there is good agreement with the observations (Figure 8b). The upper-level jet maximum magnitude (about 250 mb) in the 18Z analysis is underforecast in the model, probably owing to its reduced vertical resolution near this level. However, the height and horizontal extent of the forecast jet is in good agreement with the analysis. The model solution appears to have become 'detached' from the west lateral boundary between 850-300 mb over grid points 1 and 2. The region of weak vertical wind shear between 850 and 600 mb is still preserved in the simulation. Figure 9 shows west-to-east cross sections of the v-wind component. Note that the cross sections of v-wind display a much more complex pattern in both the analysis and forecasts than does the u-wind. Due to the limited vertical extent of the model, the 18Z forecast v-wind component above 200 mb cannot produce properly all the values seen in the analysis. However, the placement of the jet-stream level -5m/sec isotach (at 250 mb) is in good agreement with observations. The observed maximum at 600 mb in the eastern half of the cross section is reproduced in the forecast, but is about 100 mb too low. The 'patch' of winds >5m/sec above 900 mb in the analysis is forecast well. However, the simulation again shows evidence of a southerly low-level jet which is stronger than observed.

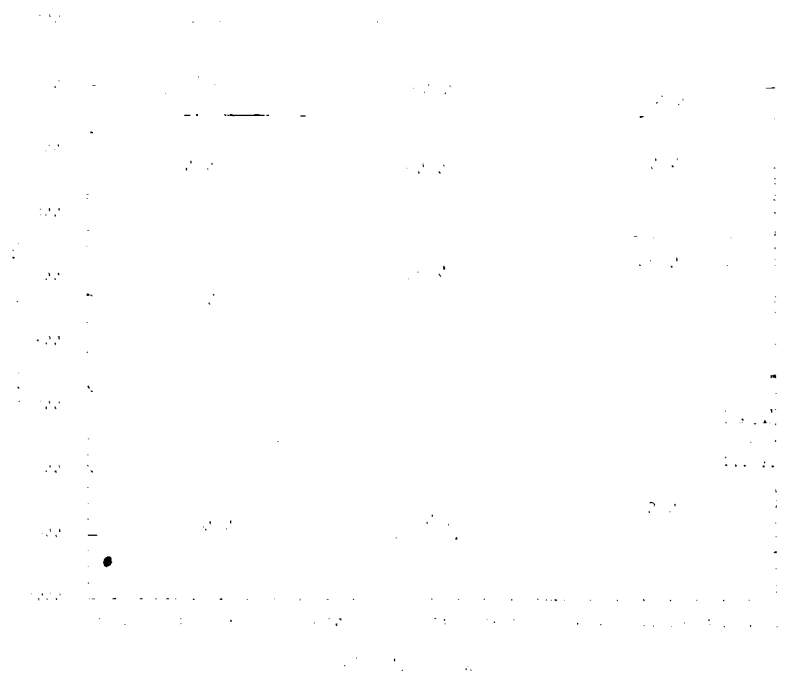


Figure 8a.

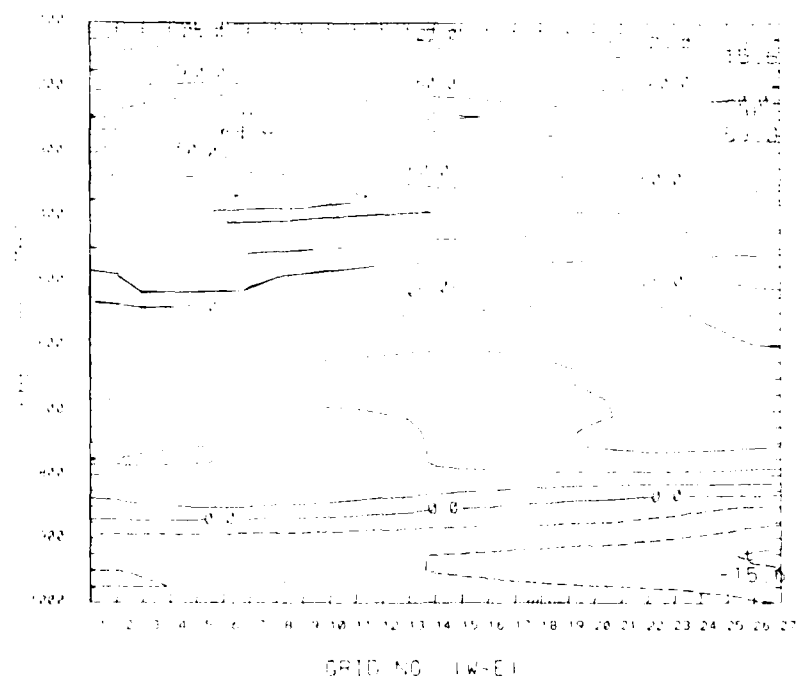


Figure 8b.

Figure 8. Vertical Cross Section of 6-h (a) Forecast and (b) Observed u-wind Component (m/sec) Valid 18Z Mar 82

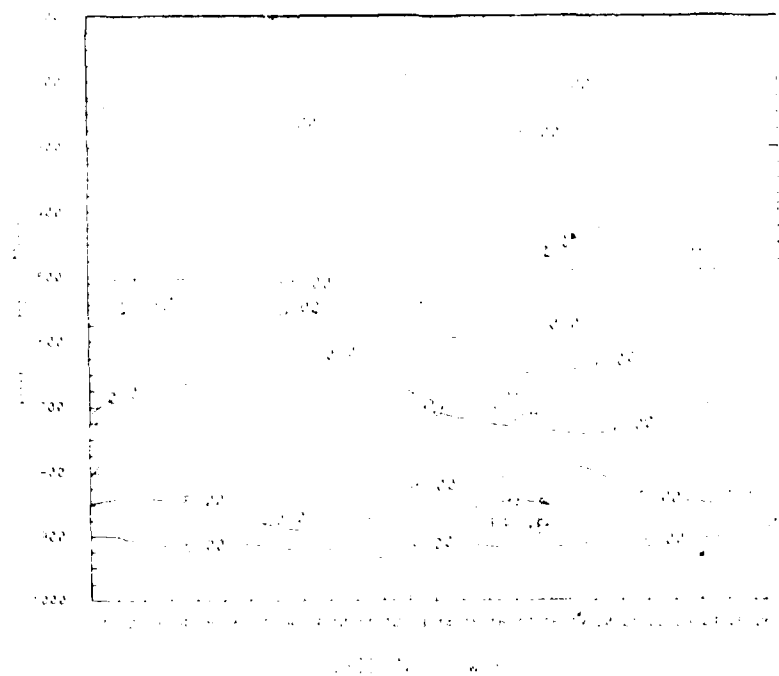


Figure 9a.

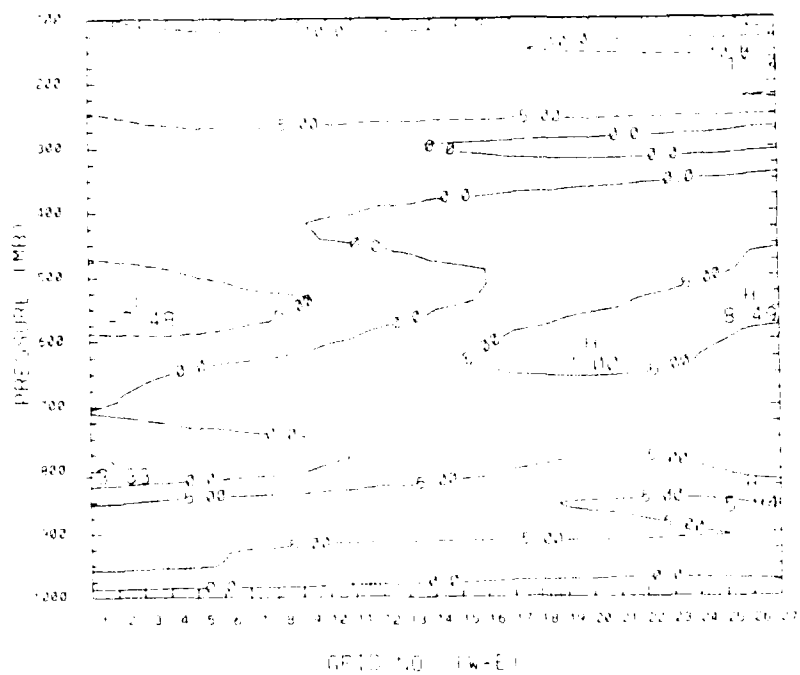


Figure 9b.

Figure 9. Vertical Cross Section of 6-h (a) Forecast and (b) Observed v-wind Component (m/sec) Valid 18Z Mar 82

In Figure 10 we begin to look at some of the mass-related variables. At level 0.9978, note that the pattern of the region bounded by the 4 degree and 6 degree C isotherms in the 18Z forecast corresponds fairly well with that in the analysis, but is forecast to be 40-100 km too far north. This might be attributable to the low precipitation rates that were produced by the model which consequently permitted the surface to warm too much. At 850 mb (Figure 11) the forecast northwest-southeast orientation of the isotherms appears to be interrupted in the central part of the domain. In particular, the forecast isotherms are distorted by the anomalously strong southerly low-level jet that is simulated by the model. At 500 mb (Figure 12), the analyzed temperature trough near the eastern boundary is smoothed in the forecast. A similar occurrence is seen in the 300 mb forecast (Figure 13).

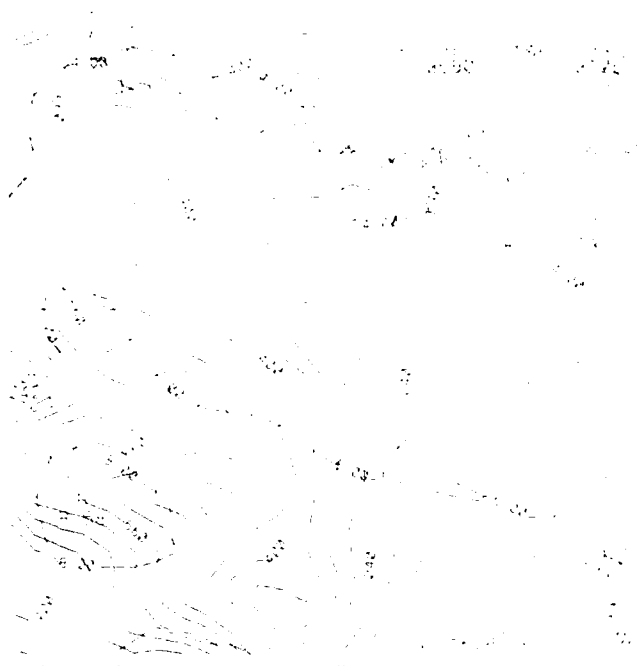


Figure 10a.

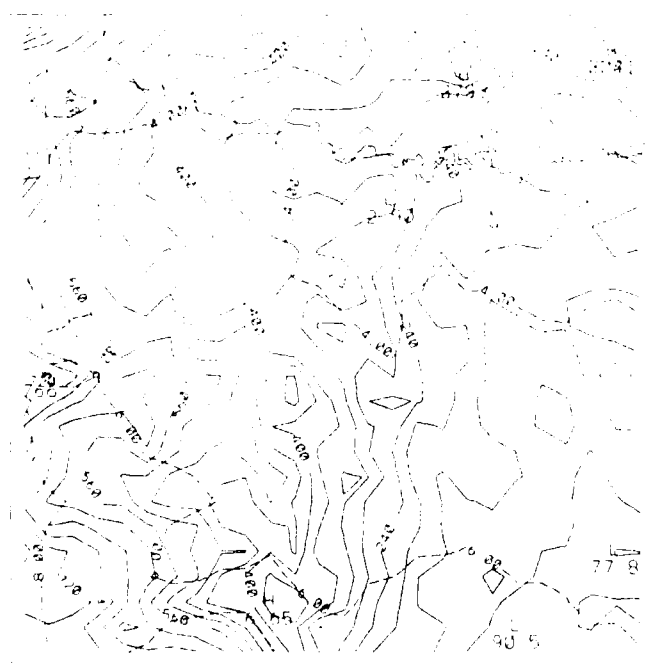


Figure 10b.

Figure 10. Horizontal Plot of 6-h (a) Forecast and (b) Observed Geopotential Height (Solid, in m) and Temperature (Dashed, in °C) for Sigma-level 0.9978 Valid 18Z Mar 82



Figure 11a.

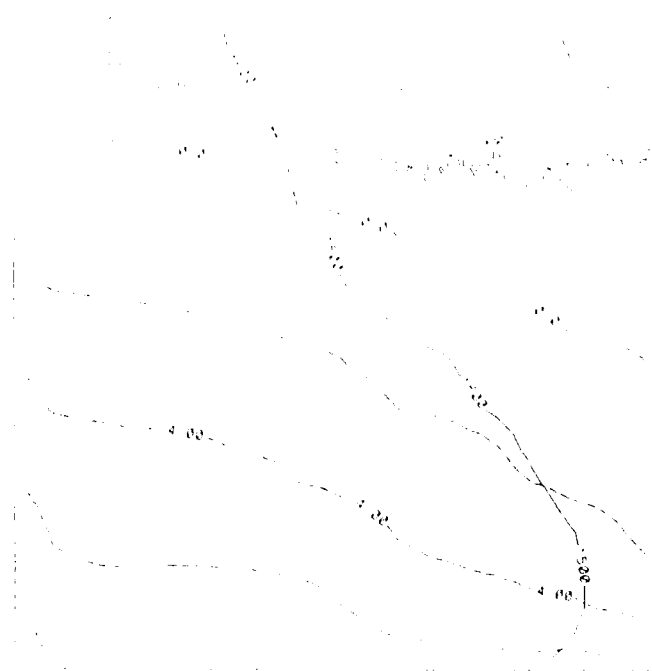


Figure 11b.

Figure 11. Horizontal Plot of 6-h (a) Forecast and (b) Observed Geopotential Height (Solid, in m) and Temperature (Dashed, in °C) for 850 mb Valid 18Z Mar 82





Figure 12a.

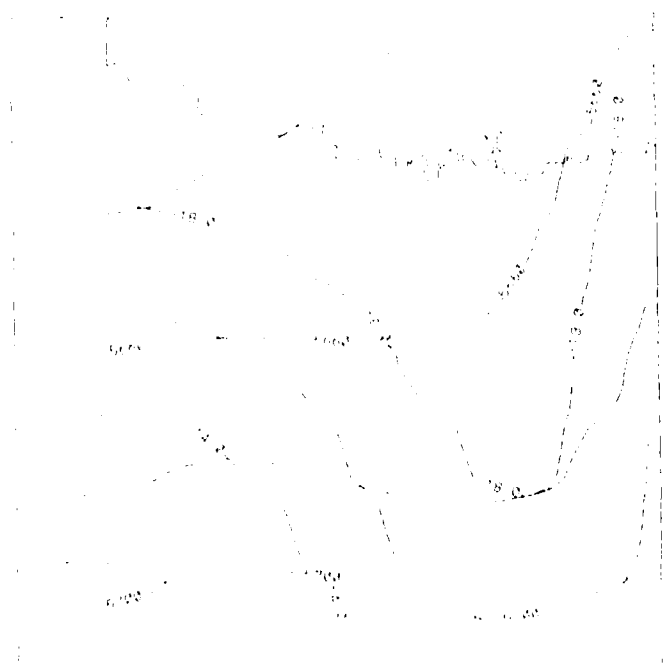


Figure 12b.

Figure 12. Horizontal Plot of 6-h (a) Forecast and (b, Observed Geopotential Height (Solid, in m) and Temperature (Dashed, in °C) for 500 mb Valid 18Z Mar 82

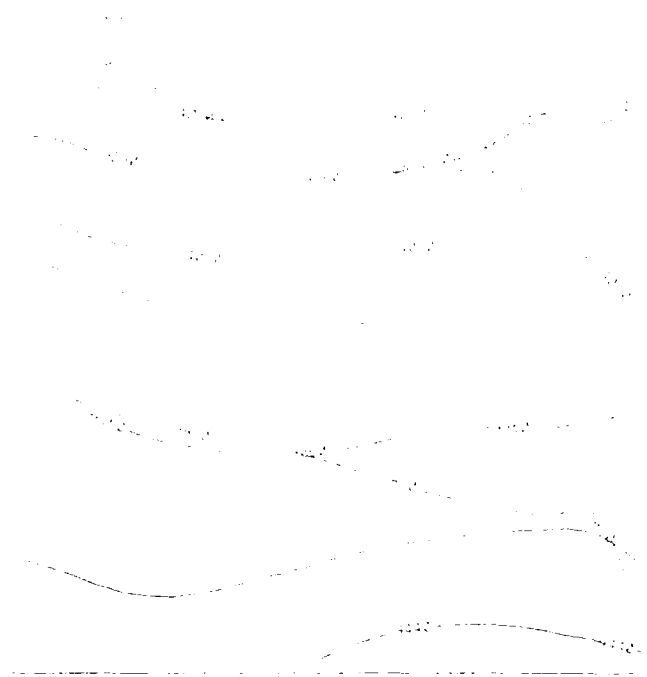


Figure 13a.

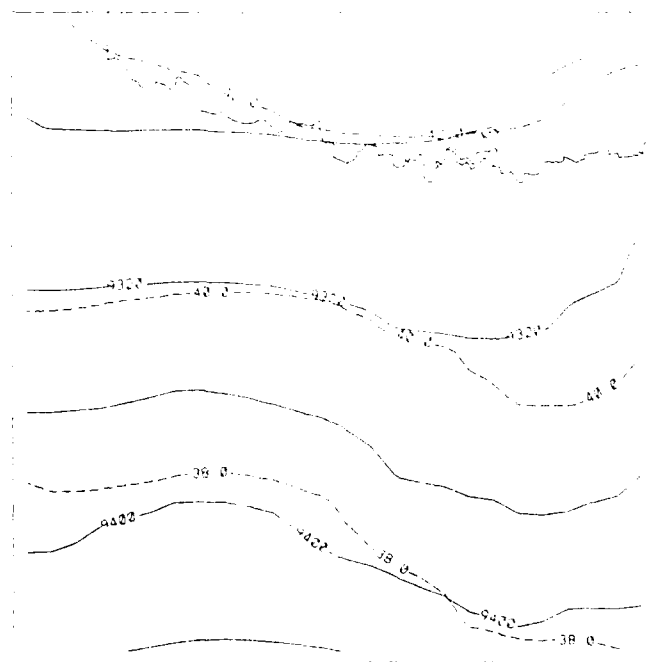


Figure 13b.

Figure 13. Horizontal Plot of 6-h (a) Forecast and (b) Observed Geopotential Height (Solid, in m) and Temperature (Dashed, in °C) for 300 mb Valid 18Z Mar 82

In Figure 14 we see a west-to-east cross section of potential temperature. The forecast (Figure 14a) generally is in good agreement with the analysis. Note that the forecast is slightly warmer than the analysis near the surface. The analyzed inversion between 900 and 800 mb is replicated in the forecast. Both the forecast and the analysis display a region of less stable air between 700 and 600 mb. Finally, the forecast height of the tropopause is consistent with observations.

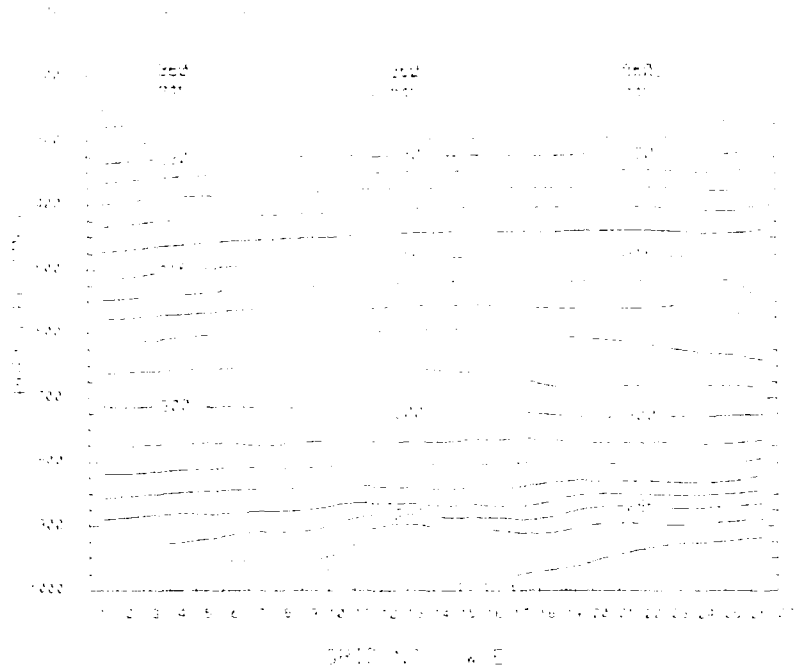


Figure 14a.

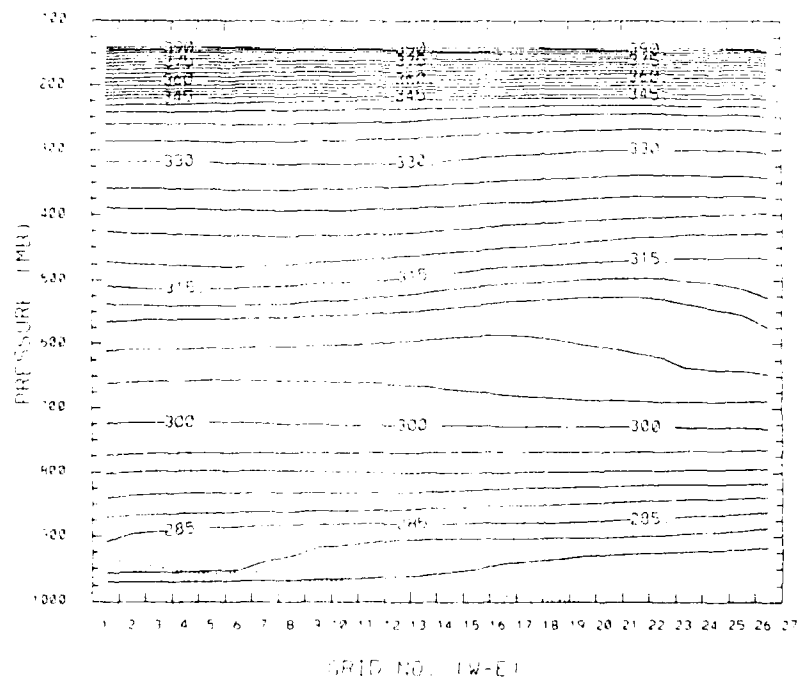
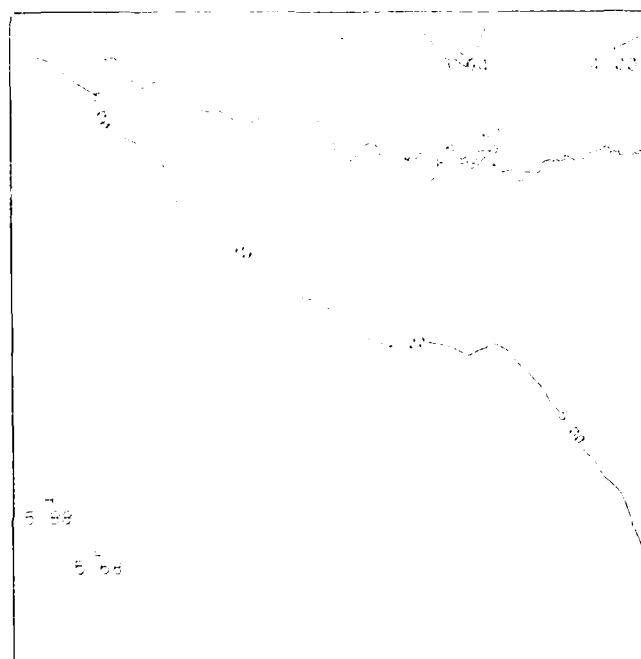


Figure 14b.

Figure 14. Vertical Cross Section of 6-h (a) Forecast and (b) Observed Potential Temperature (K) Valid 18Z Mar 82

The level 0.9978 plot of vapor mixing ratio is shown in Figure 15. The forecast 5g/kg contour at this level is similar to that in the analysis. Forecast values are too high in the southwest corner. This is probably related to the fact that in this area the values of soil moisture were initialized to be too high. At 850 mb (Figure 16) the observed ridge of  $q_v$  in the western half of the domain has been shifted eastward in the forecast. This seems to be a consequence of the forecast low-level jet which was forecast to be too strong and thus may have erroneously advected the moisture too far north. The analyzed pattern of  $q_v$  at 500 mb (Figure 17) is forecast fairly well. The east-west cross section of analyzed mixing ratio (Figure 18b) shows a dry tongue centered at about 925 mb over the eastern third of the domain that also appears in the forecast (Figure 18a). The region of  $q_v > 5$  g/kg at about 800 mb that appears in the analysis is not maintained sufficiently far from the ground in the forecast. Thus, the forecast is too moist in the immediate vicinity of the ground ( $> 5$  g/kg) over grid points 1 to 10. The vertical gradient between 700 and 600 mb in the forecast is not as sharp as that in the analysis.



**Figure 15. Horizontal Plot of 6-h (a) Forecast and (b) Observed Vapor Mixing Ratio (g/kg) Valid 18Z 27 Mar 82**



Figure 16a.

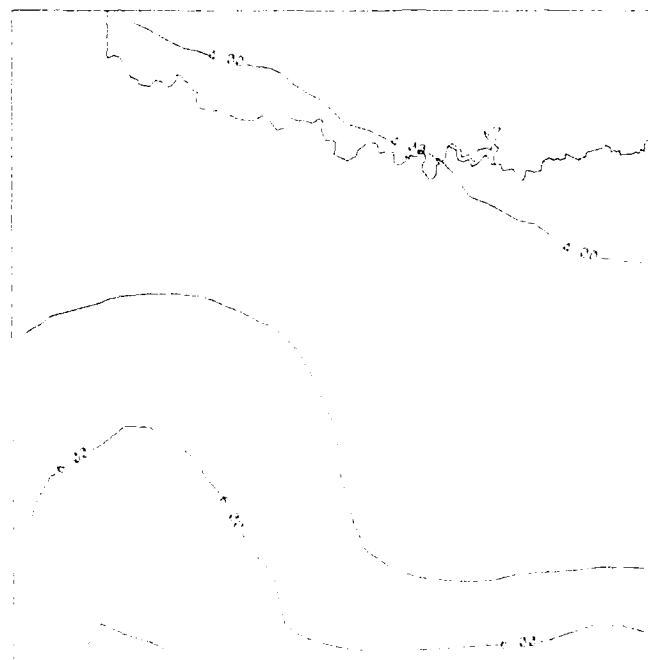


Figure 16b.

Figure 16. Horizontal Plot of 6-h (a) Forecast and (b) Observed Vapor Mixing Ratio for 850 mb Valid 18Z 27 Mar 82

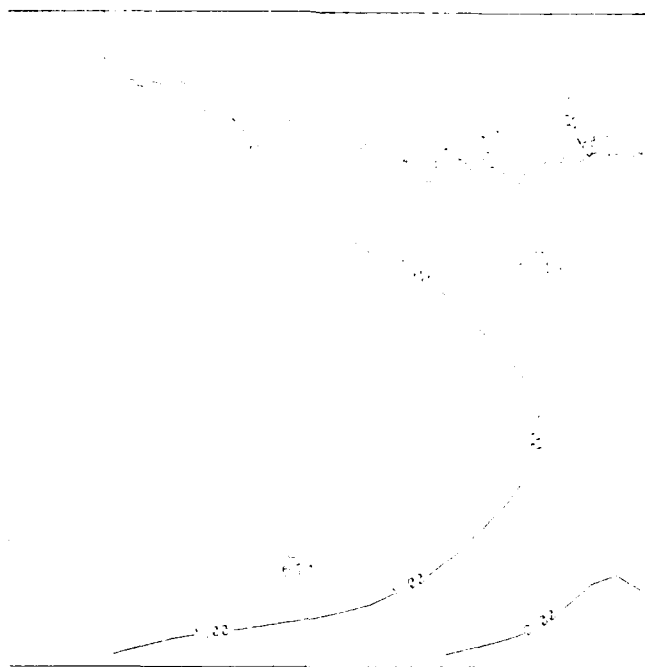


Figure 17a.

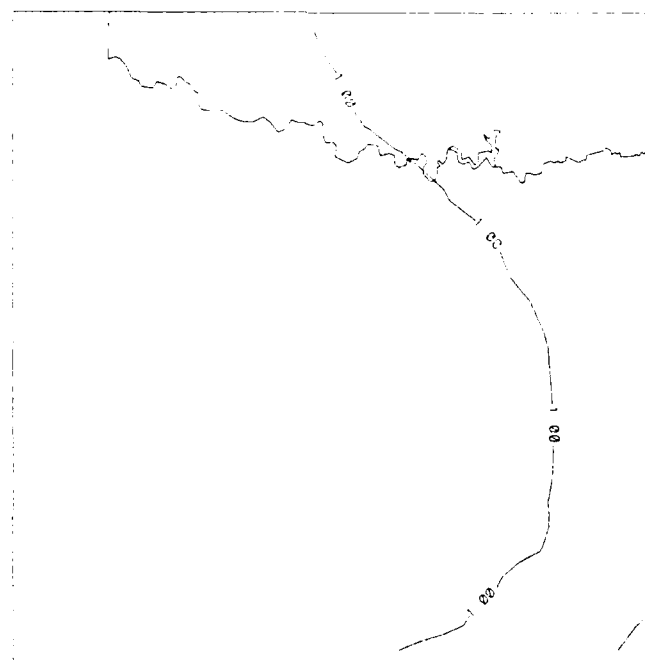


Figure 17b.

Figure 17. Horizontal Plot of 6-h (a) Forecast and (b) Observed Vapor Mixing Ratio for 500 mb Valid 18Z 27 Mar 82





Figure 18a.

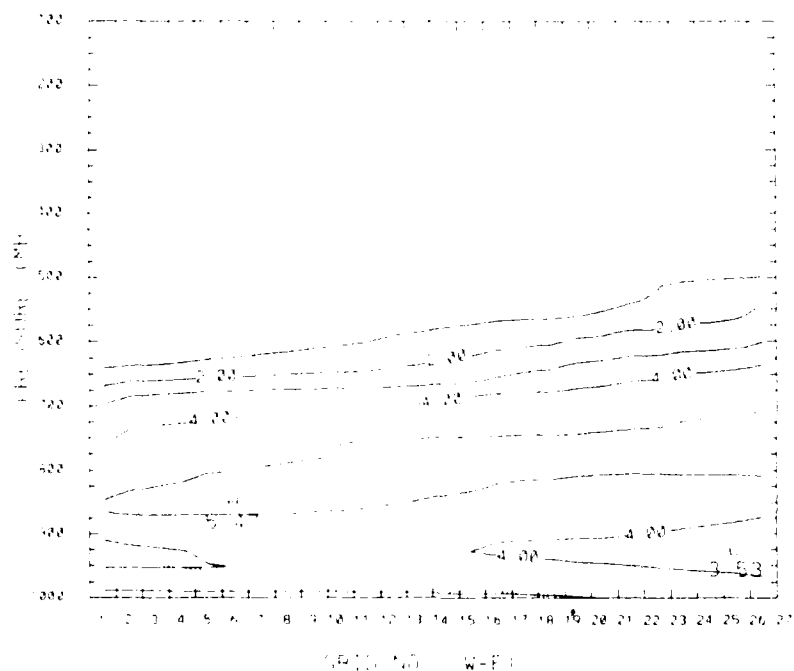


Figure 18b.

Figure 18. Vertical Cross Section of 6-h (a) Forecast and (b) Observed Vapor Mixing Ratio (g/kg) Valid 18Z 27 Mar 82

Figure 19 is an east-west cross section of forecast cloud water mixing ratio ( $q_{cw}$ ) across the center of the domain. Note the elongated structure in the  $q_{cw}$  field as the low-level air flows upslope toward the west.

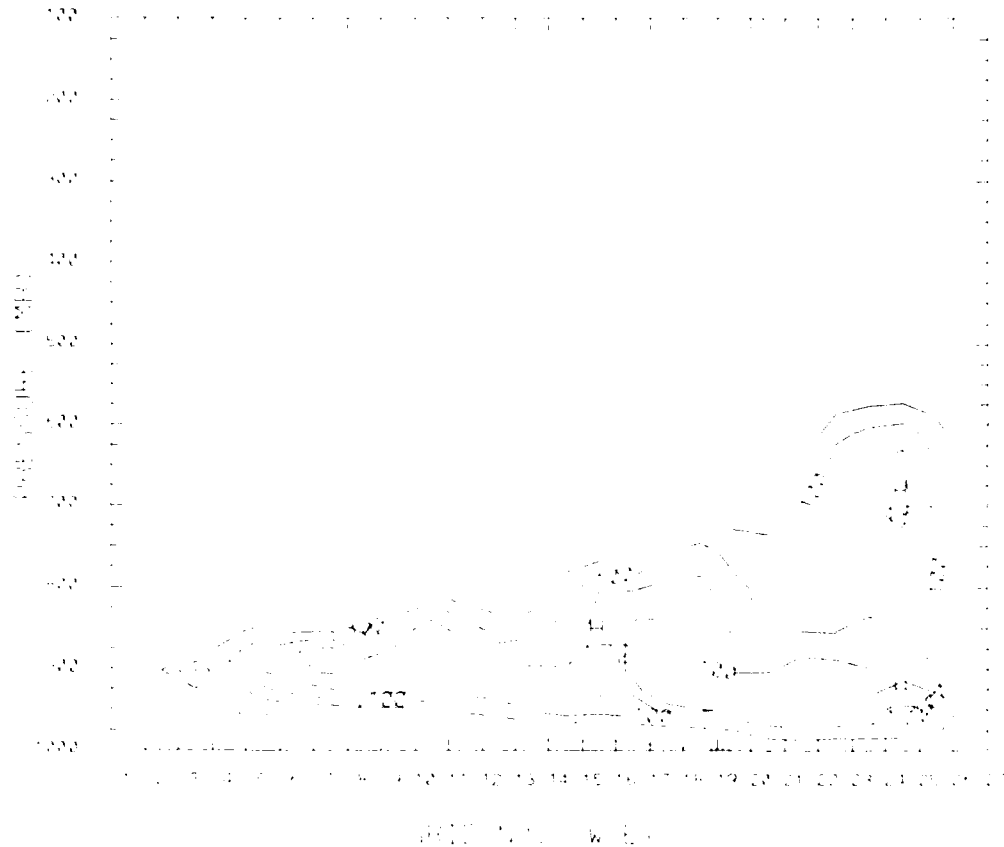
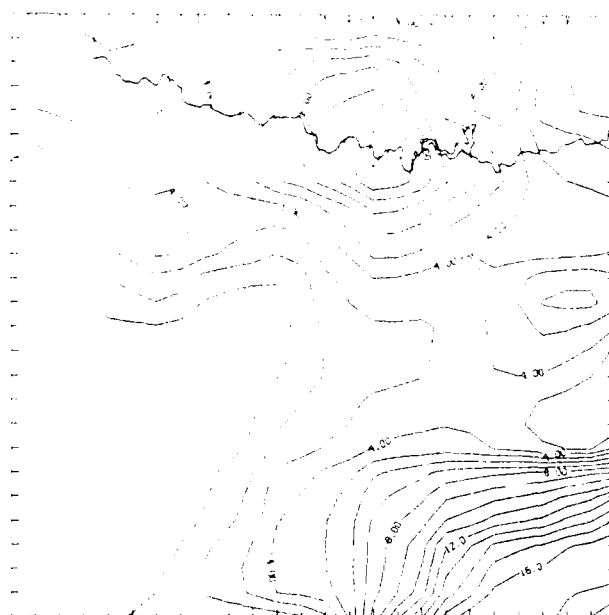


Figure 19. Vertical Cross Section of 6-h Forecast Cloud Water Mixing Ratio (g/kg) Valid 18Z 27 Mar 82

The 6-h precipitation forecast (Figure 20a) attempts to simulate the analyzed double maximum over the Red River (Figure 20b) and just to the southeast. However, overall amounts are underforecast by the model by a factor of 2 or 3. The forecast, like the analysis, displays a third maximum near the southeast corner of the domain, but amounts are grossly underforecast by the model.



**Figure 20. Horizontal Distribution of 6-h (a) Forecast and (b) Observed Precipitation (cm) Valid 18Z 27 Mar 82**

In an attempt to evaluate the aggregate impact of the PBL/soil parameterization on the forecast, the model was run without invoking the PBL code. Therefore, no surface exchanges were permitted for sensible or latent heat and momentum. In this run there also was no vertical turbulent diffusion above the surface layer.

One result was that winds at the surface became too strong (Figure 21). Note that the winds over the interior of the domain are not consistent with the winds that are specified (from observations) at and near the inflow lateral boundaries (compare with Figure 4). Figure 22 shows geopotential height and temperature near the ground surface. Comparison with Figure 10 indicates that temperatures in the no-PBL case are too cold. A likely explanation is that no sensible heat flux from the surface was available to warm the overlying air in this experiment. This experiment also revealed that the model produced about 20-50 percent less precipitation without the PBL/soil model (Figure 23). In terms of the total mass of precipitation that fell during the 6-h simulation, the precipitation decreased by 37 percent when the PBL was turned off. It appears that in the experiment with the PBL/soil model, the exchange of surface moisture into the near-surface air is important for the production of low-level clouds and subsequent precipitation. Figure 24 shows that the near-surface vapor mixing ratio for the no-PBL case is lower than that for the PBL case (Figure 15). It is important to note that, at least in this case, the availability of a surface moisture source contributed in a positive way to the low-level moistening and precipitation process. In the no-PBL case, the onset of cloud formation appears to have been delayed as the low-level clouds move upslope from east to west. This idea is reinforced by Figure 25 which shows a cross section of  $q_{cw}$  for the no-PBL case. Note that there is actually less low-level cloud (compare with Figure 19) over most of the cross section, with most near-surface cloud not forming until it is well toward the western part of the domain.

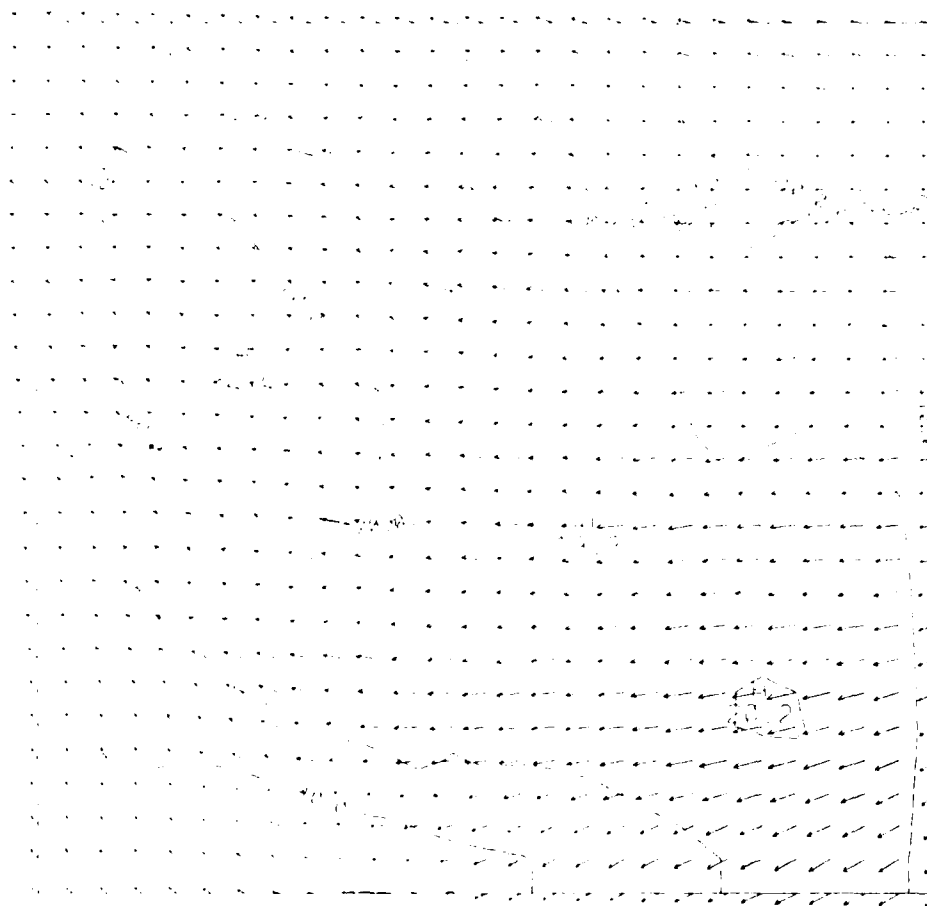


Figure 21. Horizontal Plot of 6-h Forecast Wind (m/s) at  
Sigma-level 0.9978 for Non-PBL Case Valid 18Z 27 Mar 82

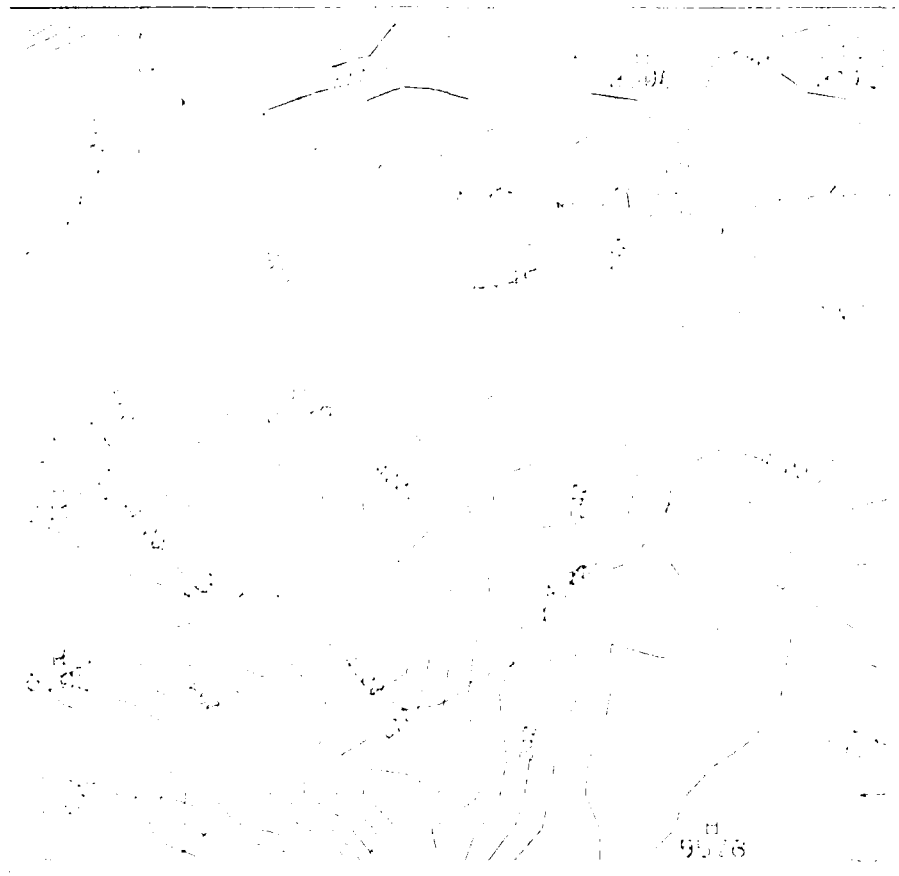
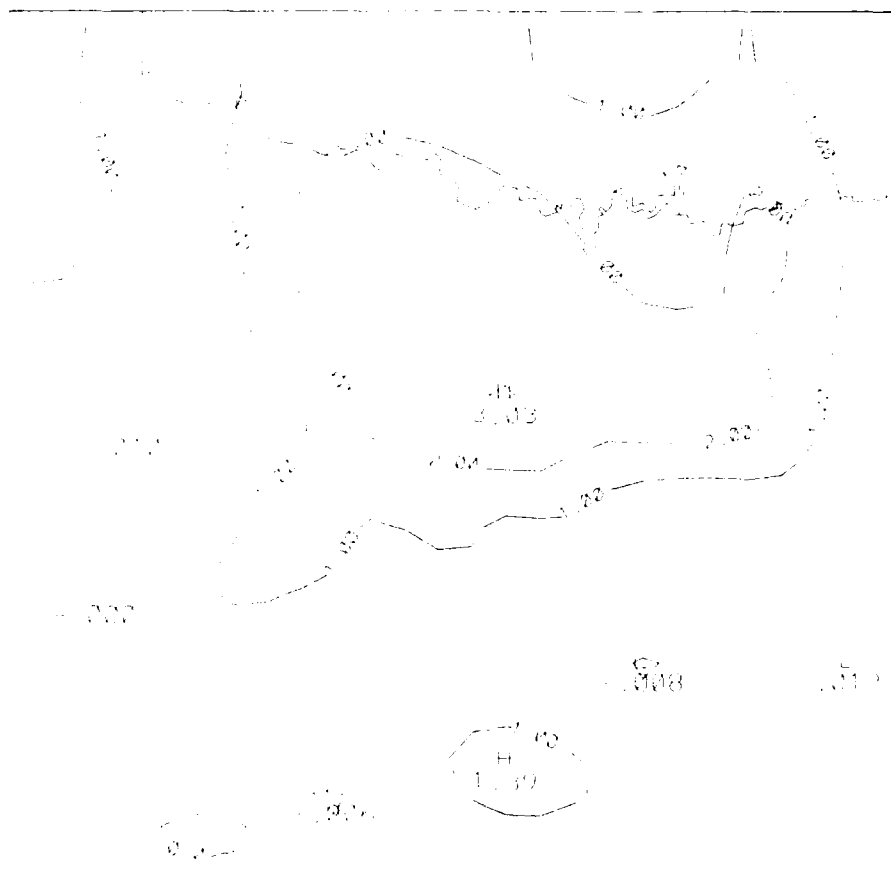
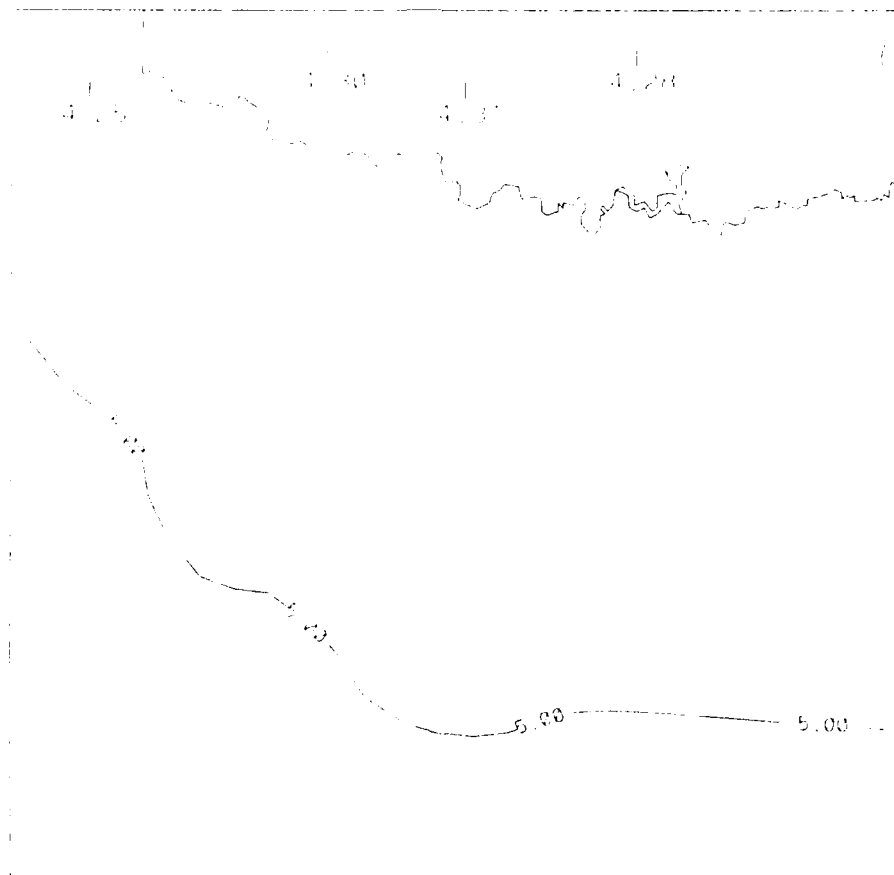


Figure 22. Horizontal Plots of 6-h Forecast Geopotential Height (Solid, in m) and Temperature (Dashed, in °C) at Sigma-level 0.9978 for Non-PBL Case Valid 18Z 27 Mar 82





**Figure 24. Horizontal Plot of 6-h Forecast Vapor Mixing Ratio (g/kg) at Sigma-level 0.9978 for Non-PBL Case Valid 18Z 27 Mar 82**



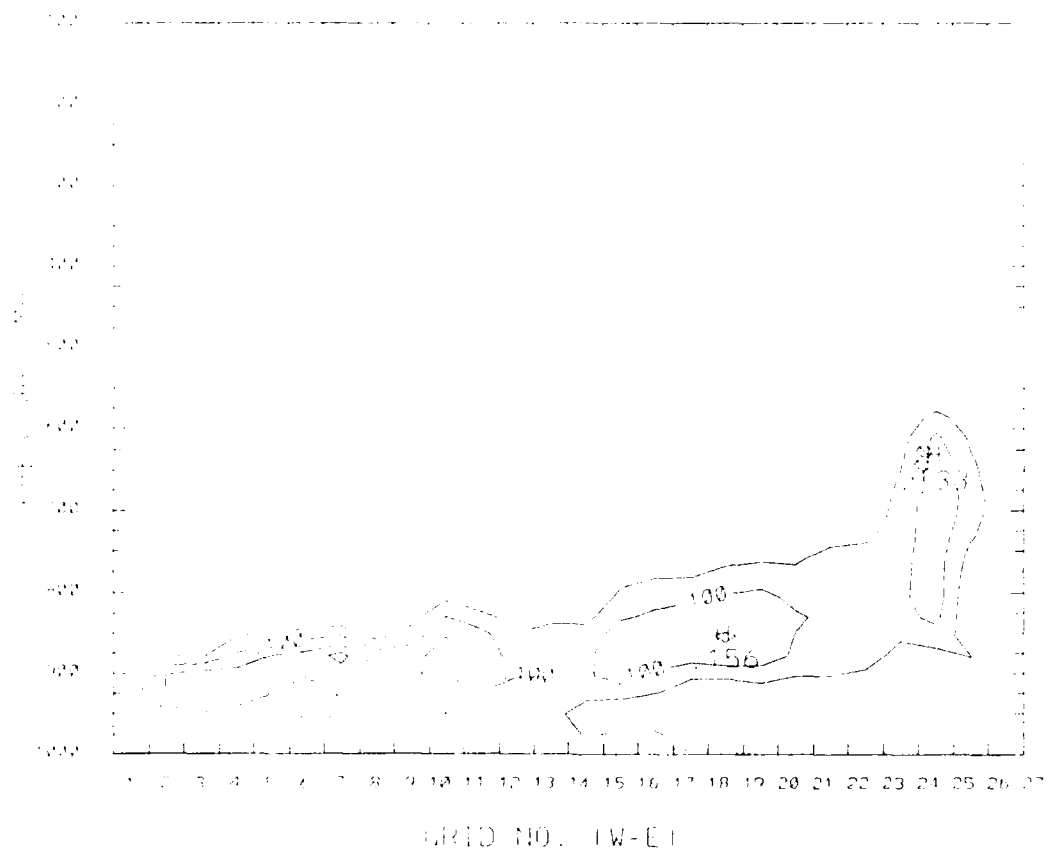


**Figure 25. Vertical Cross Section of 6-h Forecast Cloud Water Mixing Ratio (g/kg) for Non-PBL Case Valid 18Z 27 Mar 82**

At higher altitude, the model solution of the no-PBL case at 6 hours was not qualitatively different from that in the PBL case.

Several other experiments were performed to test the sensitivity of the soil/surface model to 1) the absence of moisture at the surface and 2) the absence of clouds. These results for 12-hour forecasts are presented Figure 26. In the first experiment latent heat was not permitted to affect the surface energy budget. In the second experiment ('clear') clouds were not permitted to attenuate the incoming shortwave and outgoing longwave radiation. The last experiment ('clear/dry') tests the combined effects described in the first two experiments. Finally, 'reference' refers to the original experiment with all effects included. Note in Figure 26a that ground temperatures are, by far, highest for the clear/dry case where temperatures are about 15 C higher than in the reference run. The ground temperatures for the clear case do not differ greatly from those in the dry soil run. The reference run produced the lowest surface temperatures. The model, therefore, confirms our intuitive expectations of how the presence of cloud and soil moisture affect the ground temperature. Less easily explained, however, is the curious double maximum of surface temperature in the clear/dry case. Examination of the model PBL output (not shown) reveals a complex interaction between the mean flow and the PBL mixing process at this time. Under the circumstances present in this study, this behavior is not characteristic of the real atmosphere and may be evidence of a numerical problem with the manner in which the PBL model is linked to the mesoscale model. Figure 25b shows the temporal variation of PBL height in the various experiments. Again, the clear/dry case departs significantly from the results of the other experiments and exhibits sharp changes in PBL height after 12 LST. This figure also reveals that the clear case displays oscillations similar to the clear/dry case. The curve for the reference run shows an example of PBL collapse that is much more in line with our expectations (note curve at 17-18 LST).

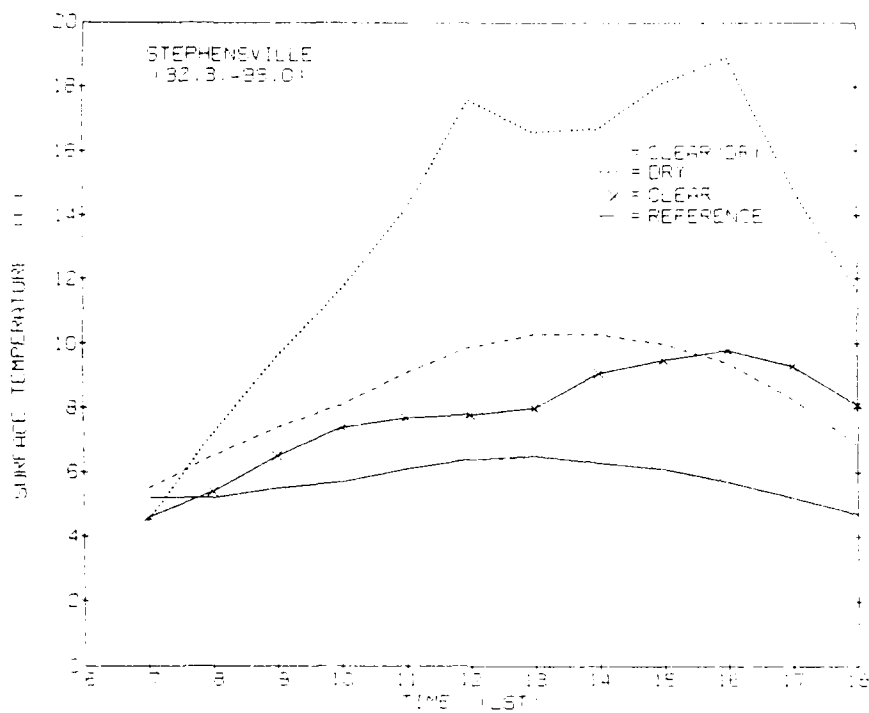


Figure 26a.

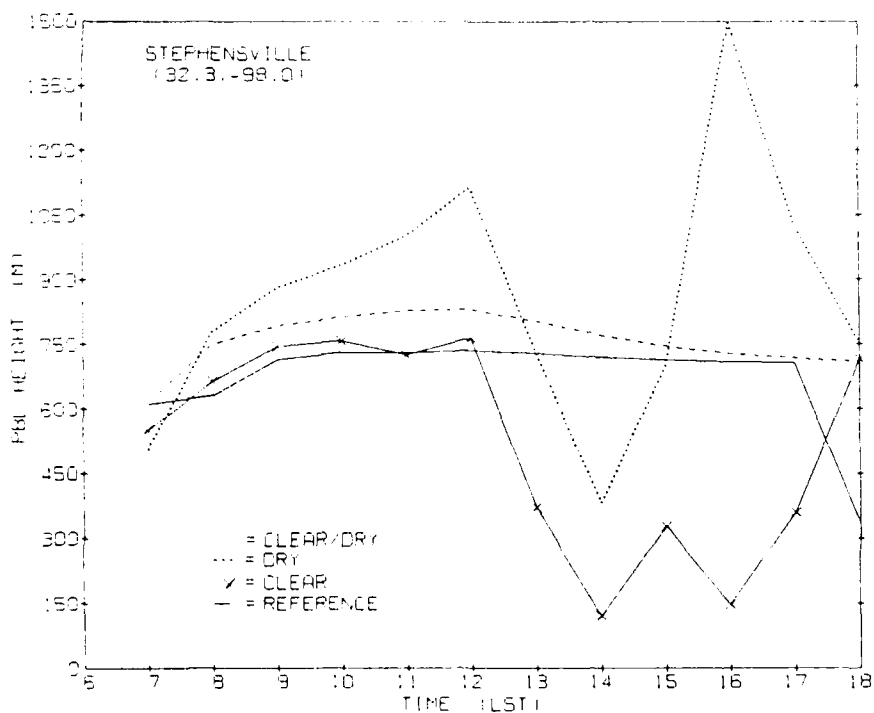


Figure 26b.

Figure 26. Plot of 12-h (a) Forecast Ground Temperature and (b) PBL Height vs. Time for Different Experiments

## 5. SUMMARY AND CONCLUSIONS

A meso-beta grid point model with a detailed microphysics parameterization of warm-cloud processes is briefly described. The model is initialized with a mesoscale data set and 6-h model predicted parameters are compared with observations. Velocity, temperature, and moisture parameters generally appeared to be forecast well. The largest discrepancies appeared at about 850 mb where the model developed too strong a southerly low-level jet. Consequently, temperature and moisture values were erroneously advected at this level, resulting in distorted forecast fields of these variables.

The model was additionally run without any PBL/soil model physics to evaluate the effect that these processes have on the forecast. The most noticeable effects were observed near the surface where forecast temperatures were too cold and winds were too high. This run also yielded about 20-50 percent less precipitation. The model's soil physics parameterization appears to be essential to represent realistically the supply to the lower atmosphere of the moisture necessary for the precipitating clouds. Qualitative aspects of this forecast at higher levels were similar to the full-PBL reference run.

Sensitivity tests with the PBL/soil model revealed that, at least for this case, the effect of soil moisture on ground temperature is approximately as important as the effect of clouds on ground temperature. However, when the effects of clouds were removed from the model atmosphere, the ground temperature and PBL height tended to exhibit unusual oscillations. The reasons for this are not yet known.

Much has been written about the positive impact of surface heating and moistening on the storm-scale environment. Our results seem to confirm that a PBL/soil model like the one tested here may be necessary to properly simulate the conditions that can lead to significant weather events.

## References

1. Nickerson, E. C. (1979) On the numerical simulation of airflow and clouds over mountainous terrain, *Bett. Atmos. Phys.*, **52**:161-177.
2. Nickerson, E. C., Richard, E., Rosset, R. and Smith, D. R. (1986) The numerical simulation of clouds, rain, and airflow over the Vosges and Black Forest Mountains: A meso-beta model with parameterized microphysics, *Mon. Wea. Rev.*, **114**:399-414.
3. Troen, I. and Mahrt, L. (1986) A simple model of the atmospheric boundary layer: sensitivity to surface evaporation, *Bound. -Layer Meteor.*, **37**:129-148.
4. Pan, H. -L. and Mahrt, L. (1987) Interaction between soil hydrology and boundary layer development, *Bound. -Layer Meteor.*, **38**:185-202.
5. Perkey, D. J. and Kreitzberg, C. W. (1976) A time-dependent lateral boundary scheme for limited-area primitive equation models, *Mon. Wea. Rev.*, **104**:744-755.
6. Barnes, S. L. (1973) *Mesoscale objective analysis using weighted time-series observations*, NOAA Tech. Memo ERL NSSL-62.
7. Yee, S. Y.- K. and Jackson, A. (1988) *Blending of surface and rawinsonde data in mesoscale objective analysis*, AFGL-TR-88-0144, ADA 203984.
8. Washington, W. M. and Baumhefner, D. P. (1975) A method for removing Lamb waves from initial data for primitive equation models. *J. Appl. Meteor.* **14**:114-119.